



HAL
open science

Impact of Mn 2+ in bisphenol A degradation by chelating agents-assisted manganese dioxide: mechanism understanding and efficiency evaluation

Daqing Jia, Marcello Brigante, Changbo Zhang, Gilles Mailhot

► To cite this version:

Daqing Jia, Marcello Brigante, Changbo Zhang, Gilles Mailhot. Impact of Mn 2+ in bisphenol A degradation by chelating agents-assisted manganese dioxide: mechanism understanding and efficiency evaluation. *Journal of Water Process Engineering*, 2023, 56, 10.1016/j.jwpe.2023.104388 . hal-04281886

HAL Id: hal-04281886

<https://uca.hal.science/hal-04281886>

Submitted on 13 Nov 2023

HAL is a multi-disciplinary open access archive for the deposit and dissemination of scientific research documents, whether they are published or not. The documents may come from teaching and research institutions in France or abroad, or from public or private research centers.

L'archive ouverte pluridisciplinaire **HAL**, est destinée au dépôt et à la diffusion de documents scientifiques de niveau recherche, publiés ou non, émanant des établissements d'enseignement et de recherche français ou étrangers, des laboratoires publics ou privés.

1 **Impact of Mn²⁺ in bisphenol A degradation by chelating agents-assisted manganese**
2 **dioxide: mechanism understanding and efficiency evaluation**

3 Daqing Jia^{a,*}, Marcello Brigante^a, Changbo Zhang^b, Gilles Mailhot^{a,*}

4 ^aUniversité Clermont Auvergne, CNRS, Clermont Auvergne INP, Institut de Chimie de Clermont-
5 Ferrand, F-63000 Clermont-Ferrand, France.

6 ^bKey Laboratory of Original Agro-Environmental Pollution Prevention and Control, Agro-
7 Environmental Protection Institute, Ministry of Agriculture and Rural Affairs, P. R. China, Tianjin,
8 300191, China.

9

10 *Corresponding author: gilles.mailhot@uca.fr

11 *Corresponding author: daqing.jia@uca.fr

12

13

14

15

16

17

18

19

20

21

22

23

24

25

26 Keywords: Manganese oxides, ligands, manganese ions, complexation, water treatment

27

1 **Abstract**

2 Manganese dioxide (MnO_2) is popular in eliminating organic pollutants in water. The
3 application of chelating agents to enhance the reactivity of MnO_2 has been previously
4 reported. Much attention has been taken to increase the amount of Mn(III) species in the
5 manganese oxide/ligands system to achieve a higher degradation. However, the role of Mn^{2+}
6 is rarely studied. In this study, the efficiency and mechanism of bisphenol A (BPA)
7 degradation by pyrophosphate (PP)-assisted MnO_2 in the presence of Mn^{2+} was investigated.
8 The results show that 25 μM of BPA can be completely removed by the $\text{MnO}_2/\text{PP}/\text{Mn}^{2+}$
9 system in 90 min. Increasing PP and Mn^{2+} concentrations effectively improved the
10 degradation of BPA. The primary reactive species for the degradation of BPA was determined
11 to be the Mn(III)-PP complex. Moreover, Mn^{2+} were verified to play the bridging, reductive,
12 and catalytic roles to enhance the degradation of BPA. Furthermore, the substituted ligands
13 such as nitrilotriacetic acid (NTA) and ethylenediaminetetraacetic acid disodium salt hydrate
14 (EDTA) were verified to exhibit higher activity than citrate on MnO_2 activation in the
15 presence of Mn^{2+} . The adaptability of the proposed system was evaluated in various
16 conditions such as the presence of metal cations or inorganic ions and wide solution pH range.
17 In addition, the performance of $\text{MnO}_2/\text{PP}/\text{Mn}^{2+}$ system on BPA removal in the sewage
18 treatment plant outlet water was evaluated as well. These findings highlight the positive role
19 of Mn^{2+} in the system of MnO_2 /ligands and provide a practical reference for the application of
20 ligands-assisted manganese oxides in wastewater treatment.

21

22

23

1 **1 Introduction**

2 Manganese oxides are one common transition metal-based minerals, which possess various
3 oxidation states [1]. The application of manganese oxides in dealing with different organic
4 pollutants in waters has become one popular water treatment technology [2]. High-valent
5 manganese oxides such as $\text{Mn}^{\text{IV}}\text{O}_2$, $\text{Mn}^{\text{VII}}\text{O}_4^-$ can directly oxidize most organic contaminants
6 through the electron exchange processes [3,4]. However, the low-valent manganese oxides
7 including $\text{Mn}_2^{\text{III}}\text{O}_3$, $\text{Mn}^{\text{III}}\text{OOH}$, $\text{Mn}^{\text{II}}\text{O}$ exhibit weak ability to oxidize organic contaminants,
8 although Mn^{III} species were reported to have higher reduction potential ($E_{\text{Mn}^{3+}/\text{Mn}^{2+}} = 1.54 \text{ V}$
9 vs Normal Hydrogen Electrode (NHE)) than MnO_2 ($E_{\text{Mn}^{4+}/\text{Mn}^{2+}} = 1.24 \text{ V vs NHE}$) [5–7]. To
10 improve the reactivities of all-valence manganese oxides, various radical precursors (e.g.,
11 hydrogen peroxide (H_2O_2), persulfate, and bisulfite) have been employed to generate different
12 oxidative radicals and high-valence manganese species (e.g., Mn(IV), Mn(V)). For instance,
13 Huang et al. reported the efficient degradation of bisphenol A (BPA) by MnO_2 -activated
14 peroxymonosulfate (PMS) through the generation of sulfate radicals ($\text{SO}_4^{\bullet-}$) [8]. Jia et al.
15 elucidated the positive role of generated Mn(IV) species in the manganite/PMS system for the
16 degradation of estrogenic compounds [9].

17 The use of ligands in the transition metal-based advanced oxidation process (AOPs) to
18 improve the degradation efficiency of organic pollutants has been widely reported [10].
19 Ligands can complex transition metal ions to form stable metal ion-ligand complexes,
20 avoiding the precipitation of metal ions and broadening the applicable pH range of the system
21 [11]. One classical representative of the ligands-assisted AOPs technology is the chelate-
22 modified Fenton/Fenton-like reactions. For example, Jia et al. demonstrated the improved
23 degradation of trichloroethylene in groundwater by Fe_3O_4 -activated H_2O_2 with the addition of
24 different ligands (e.g., ethylenediaminetetraacetic acid (EDTA) and nitrilotriacetic acid
25 (NTA)) [12]. The application of ligands in the homogeneous and heterogeneous manganese-

1 based AOPs (Mn-AOPs) for removing different organic pollutants has also been reported. For
2 instance, Gao et al. reported the efficient degradation of p-nitrophenol using Mn(II) activated
3 PMS in the presence of NTA and EDTA [13]. In addition, Gao et al. found that the oxidation
4 rate of triclosan by permanganate was accelerated with the addition of several ligands,
5 including pyrophosphate (PP), NTA, and humic acid (HA) [14].

6 The principal goal of employing ligands in the Mn-AOPs is to obtain more stable Mn(III)-
7 ligand (Mn(III)-L) complexes. This can be explained by two reasons. Firstly, ligands-
8 stabilized Mn(III) species can directly oxidize organic pollutants, enhancing the degradation
9 efficiency of contaminants [15]. Secondly, ligands-stabilized Mn(III) species can provide
10 more opportunities to form higher valent Mn such as Mn(IV) and Mn(V), improving the
11 oxidation efficiency of pollutants and promoting the cycling of Mn species [13]. However, the
12 generation of Mn(III)-L complexes strongly depends on the types of participating complexing
13 agents and manganese oxides. It is reported that inorganic ligands such as pyrophosphate can
14 react with MnO₂ and manganite (MnOOH) to generate soluble Mn(III)-PP species through the
15 ligands-assisted dissolution processes [16,17]. However, the amino carboxylic ligands such as
16 NTA and EDTA only can form Mn(II)-L species with manganite [17]. Therefore, the
17 application of appropriate ligands provides a novel and effective approach to enhance the
18 reactivity of manganese oxides.

19 Dissolved divalent manganese ions (Mn²⁺) are ubiquitous in the natural aquatic environment
20 [18]. Mn²⁺, as the essential Mn species, can be oxidized to high valent manganese oxides such
21 as Mn₂O₃, MnO₂, and [MnO₄]⁻. Similarly, in the manganese oxides-participated redox
22 reactions, Mn²⁺ will be produced as the basic form of Mn species. Therefore, Mn²⁺ widely
23 exists in different waters such as the natural waters and wastewaters. The influence of Mn²⁺
24 on the reactivity of manganese dioxides has been investigated. The impact of Mn²⁺ can be
25 described from several aspects including transforming the crystal structure of MnO₂,

1 destabilizing the aggregation of MnO₂ nanoparticles in solution, and suppressing the oxidative
2 reactivity of MnO₂. For example, Elzinga reported that MnO₂ could be transformed into
3 feitknechtite (β -Mn^{III}OOH) and manganite (γ -Mn^{III}OOH) by aqueous Mn²⁺ at pH 7.5 via the
4 interfacial electron transformation [19]. Lefkowitz et al. introduced the mineralogical
5 transformation of hexagonal MnO₂ by Mn²⁺, where manganite was formed when the solution
6 pH was kept at 7.0-8.0 [20]. Cheng et al. demonstrated that the presence of Mn²⁺ in solution is
7 highly efficient in decreasing the stability of MnO₂ nanoparticles [21]. Huang et al. indicated
8 that the kinetic constant of m-aminophenol degradation was decreased from $1.04 \times 10^{-3} \mu\text{M}^{-1}$
9 min^{-1} to $0.84 \times 10^{-3} \mu\text{M}^{-1} \text{min}^{-1}$ with the addition of Mn²⁺ from 0 to 7 mM [22]. Therefore, the
10 treatment of organic pollutants by MnO₂ in the presence of metal ions such as Mn²⁺ is a
11 challenge. Moreover, extensive research has been conducted on the reactions between Mn²⁺
12 and MnO₂, ligands and MnO₂, as well as organic compounds and MnO₂. However, the
13 efficiency and underlying mechanisms of organic pollutants degradation by the
14 MnO₂/ligands/Mn²⁺ system have been scarcely reported in the literature. Sun et al. reported
15 the rapid BPA degradation by the soluble Mn(III) species at circumneutral pH with the
16 formation of fourteen BPA degradation products [23]. Qin et al. demonstrated the removal of
17 2,4-dicholophenol (2,4-DCP) using the Mn(VII)/PP/Mn²⁺ system [15]. The results showed
18 that the addition of Mn²⁺ improved the degradation of 2,4-DCP by the PP-complexed
19 Mn(VII). However, the previous studies primarily emphasized the significance of Mn(III)
20 species in the removal of contaminants. However, the role of Mn²⁺ in the context of the
21 ligand-assisted MnO₂ system is rarely studied and and if it is without enough details to
22 understand the exact roles of Mn²⁺.

23 In the current investigation, Bisphenol A was employed as a representative compound owing
24 to its substantial reactivity with acid birnessite (MnO₂) and the existence of a well-
25 documented redox mechanism that underpins the reaction [24]. The effect of PP and Mn²⁺

1 concentrations on the reactivity of MnO_2 was firstly evaluated. Two suitable concentrations
2 were selected for the following experiments. The main reactive species and the role of Mn^{2+}
3 in the $\text{MnO}_2/\text{PP}/\text{Mn}^{2+}$ system was emphatically investigated. Furthermore, various ligands,
4 namely NTA, EDTA, and citrate, were employed to examine the reactivity of MnO_2 in the
5 presence of Mn^{2+} . The impact of critical parameters, such as solution pH and the presence of
6 inorganic anions, were also assessed. Subsequently, the efficiency of the proposed system in
7 degrading BPA in actual sewage treatment plant outlet water was evaluated. The findings of
8 this study accentuate the advantageous role of Mn^{2+} in the $\text{MnO}_2/\text{ligand}$ system and provide a
9 valuable reference for the treatment of organic contaminants in ligands-assisted manganese
10 oxides system.

11

12 **2 Materials and methods**

13 **2.1 Materials**

14 Manganese (II) sulfate monohydrate, bisphenol A, ethylenediaminetetraacetic acid disodium
15 salt hydrate (EDTA), nitrilotriacetic acid (NTA), trisodium citrate dihydrate, sodium sulfate,
16 calcium chloride dehydrate, copper sulfate pentahydrate, sodium nitrate, sodium bicarbonate,
17 sodium chloride, ferrous sulfate, and *L*-ascorbic acid were purchased from Sigma-Aldrich,
18 France and were all of analytical reagents grade. Potassium pyrophosphate (96%) was bought
19 from Alfa Aesar. All chemicals were used as received without further purification. All
20 solutions were prepared in ultrapure water obtained from a water purification system
21 (Millipore, resistivity 18.2 $\text{M}\Omega$ cm).

22 **2.2 Synthesis and characterization of acid birnessite**

23 Acid birnessite (MnO_2) was synthesized using the method proposed by McKenzie [25]. The
24 synthesis process involved adding 166 mL of concentrated hydrochloric acid (HCl) dropwise

1 to 2.5 L of KMnO_4 (0.4 M) while maintaining the temperature of the suspension at 90°C .
2 After 10 minutes of reaction at 90°C , the slurry was stirred vigorously at room temperature
3 for 15 hours. The resulting precipitate was collected through centrifugation and washed with
4 ultrapure water until the conductivity reached $0.6 \mu\text{S cm}^{-1}$. The acid birnessite was stored in
5 polypropylene containers in the form of a suspension at 4°C for further use. The acid
6 birnessite was characterized using X-ray powder diffraction (XRD), Brunauer-Emmett-Teller
7 (BET), Scanning Electron Microscope (SEM), and High-Resolution Transmission Electron
8 Microscope (HRTEM). Further details regarding the characterization conditions and results
9 can be found in the Supplementary Materials (SM, Fig. S8).

10 **2.3 Kinetic experiments and analysis**

11 The chemical reactions were performed in a borosilicate brown bottle in which 50 mL of
12 solution was kept at room temperature ($298 \pm 2 \text{ K}$) under stirring (350 rpm) to ensure
13 homogeneity. $25 \mu\text{M}$ BPA was added into the 50 mL reaction solution containing a certain
14 concentration of PP and Mn^{2+} , then the solution pH was adjusted to the desired value using
15 NaOH (0.1 M) and HClO_4 (0.1 M). At last, manganese dioxide (MnO_2 , $230 \mu\text{M}$) was added to
16 start the reaction. 1 mL of sample was withdrawn at the predetermined interval times and was
17 immediately mixed with $20 \mu\text{L}$ *L*-ascorbic acid (0.5 M) to quench the reaction. The samples
18 were filtered by a $0.20 \mu\text{m}$ H-PTFE filter and then analyzed by HPLC.

19 BPA concentration was determined using a high-performance liquid chromatography system
20 (HPLC) equipped with a diode array detector (DAD, waters 2998). Chromatographic
21 separation (Waters 2695) was performed using a NUCLEODUR 100-3 C18 column ($150 \times$
22 4.6 mm , 5 mm of particle size, MACHEREY-NAGEL). The detection wavelength of BPA was
23 set at 225 nm (one of the absorption maxima of BPA), and the column temperature was kept
24 at 30°C . Acetonitrile (CARLO ERBA Reagents) and water (with 0.1% acetic acid) were
25 mixed as the mobile phases with a volume ratio of 60/40, and the flow rate was set at 1.0 mL

1 min⁻¹.

2 The pseudo-first-order rate constant of BPA (k_{BPA}) was calculated based on the slope of
3 $\ln(C_t/C_0)$ vs reaction time as following $\ln \frac{C_t}{C_0} = k_{\text{BPA}} \times t$ where C_0 and C_t are the initial and time
4 t concentration of BPA in the solution.

5 Mn(III)-PP solution was prepared following the procedures of Qian et al. [26]. Briefly, a
6 certain amount of potassium pyrophosphate was first dissolved in ultrapure water to achieve
7 the concentration of 5 mM, and the solution pH was adjusted to 6.0. A suitable amount of
8 Mn(III) acetate dehydrate was then added to the prepared PP solution under vigorous stirring
9 to form 1 mM of Mn(III)-PP complex. According to the need of study, the molar ratio of PP
10 and Mn(III) always keeps at 5:1 to maintain the state of complexation. The final pH of the
11 mixture solution was around 5.0. Before using, Mn(III)-PP solution was filtered through a
12 0.22 μm H-PTFE filter to remove any potential particles. Mn(III)-PP complexes was
13 measured on the UV-visible spectrophotometer (Varian Cary 3) at 480 nm and quantified
14 using the calibration curve (Fig. S1).

15 The complexe of Mn(III)-EDTA was monitored using a UV-visible spectrophotometer (Varian
16 Cary 3) at wavelengths of 488 nm to track its change over the course of the reaction [27].

17 Sewage treatment plant (STP) outlet water was collected from one wastewater treatment plant
18 named “3 rivières” (on June 2022, Clermont-Ferrand, France) and used after the filtration by
19 0.45 μm PTFE filter. The main physicochemical characteristics of STP outlet water are
20 reported in Table S1.

21

3 Results and discussion

3.1 Reactivity of MnO_2 with PP in the presence of Mn^{2+}

The adsorption of BPA on MnO_2 was verified and as mentioned in a previous article it remains negligible [28]. The degradation of BPA by PP complexed manganese dioxide (MnO_2) in the presence of Mn^{2+} was investigated. Fig. 1 shows that ~ 66% of BPA was removed by MnO_2 alone in 180 min, which can be explained by the high oxidation potential of MnO_2 [6]. The addition of PP obviously accelerated the degradation of BPA by MnO_2 (100% BPA removal in 120 min). This might be attributed to the generation of oxidative Mn(III)-PP complexes [16]. More details about the degradation processes of BPA by the MnO_2 /PP system will be discussed in *section 3.3 & 3.4*.

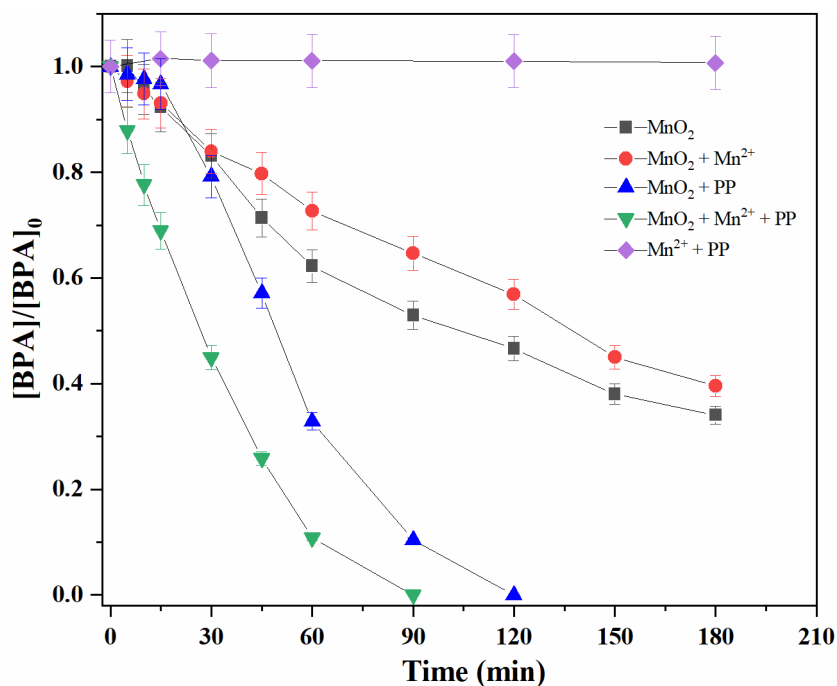


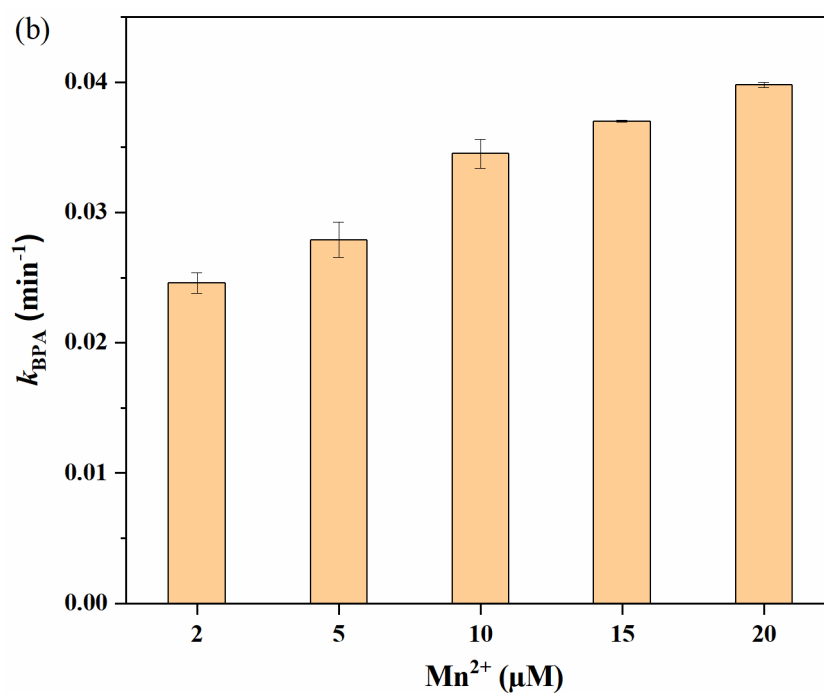
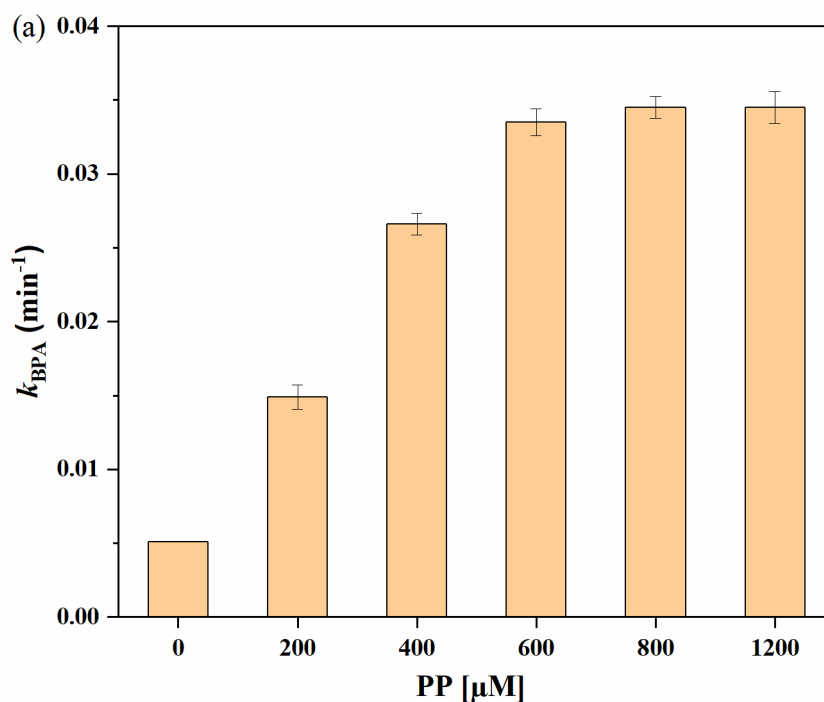
Fig. 1. BPA degradation by the MnO_2 /PP system in the presence of Mn^{2+} . Experimental conditions: $[\text{MnO}_2] = 230 \mu\text{M}$, $[\text{Mn}^{2+}] = 10 \mu\text{M}$, $[\text{PP}] = 1.2 \text{ mM}$, $[\text{BPA}] = 25 \mu\text{M}$, $\text{pH} = 5.0$. The relative experimental error lies at 5% for BPA.

Moreover, the effect of Mn^{2+} on the reactivity of MnO_2 in the presence of PP was investigated. It can be seen that an improved BPA degradation by MnO_2 /PP system was

1 achieved by adding 10 μM of Mn^{2+} (100% BPA degradation in 90 min). As a comparison, in
2 the absence of PP, the degradation of BPA by MnO_2 was slightly decreased with the addition
3 of Mn^{2+} due to the competition between Mn^{2+} and BPA for the reactive sites of MnO_2 .
4 Moreover, the blank experiment showed that the reaction of Mn^{2+} and PP achieved no BPA
5 degradation. Therefore, the presence of PP reversed the role of Mn^{2+} on the reactivity of
6 MnO_2 , promoting the degradation of BPA instead of inhibiting the removal of BPA.

7 **3.2 Effects of PP and Mn^{2+} concentrations**

8 The effects of PP and Mn^{2+} concentrations on the degradation of BPA by MnO_2 were
9 investigated. As shown in Fig. 2(a), the kinetic constants of BPA degradation (k_{BPA}) were
10 increased from 0.0051 min^{-1} to 0.0335 min^{-1} with the increase of PP concentrations from 0 to
11 $600 \mu\text{M}$. The results might be explained by the improved formation of Mn(III)-PP complexes
12 with the increase of PP dosages. However, with the continuously increasing PP concentration
13 to $1200 \mu\text{M}$, the k_{BPA} did not change much. This conclusion is consistent with the findings of
14 Zhong et al. that increasing PP concentration from 100 to $400 \mu\text{M}$, the kinetic constants of
15 pentachlorophenol degradation by the $\text{MnO}_4^-/\text{Mn(III)-PP}$ system kept stable since the excess
16 PP has no effect on the reactivity [29].



1

2

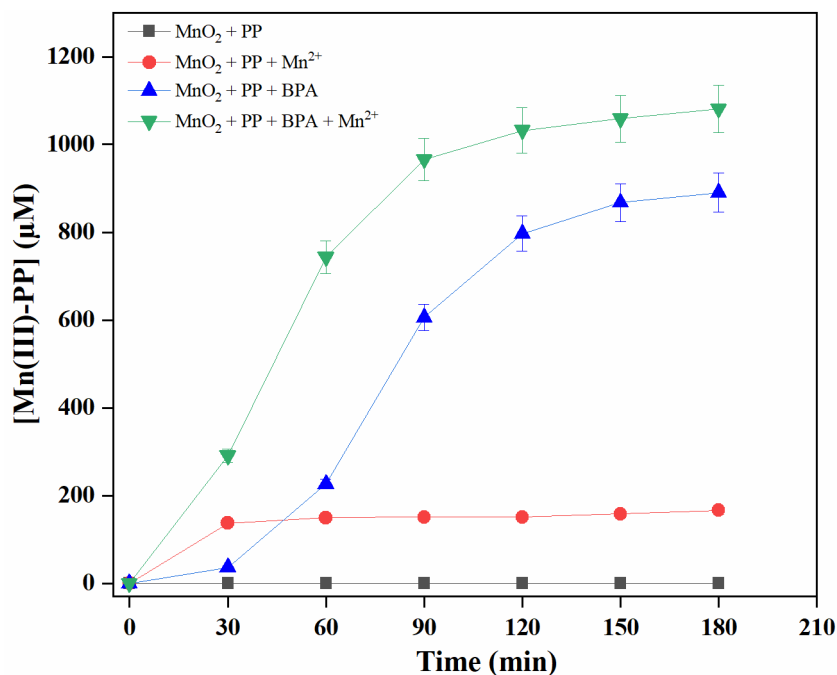
3 **Fig. 2.** Degradation of BPA (k_{BPA}) in the system of $\text{MnO}_2/\text{PP}/\text{Mn}^{2+}$. (a) Effect of PP
 4 concentrations in the presence of $10 \mu\text{M Mn}^{2+}$. (b) Effect of Mn^{2+} concentrations using 1.2
 5 mM PP. $[\text{MnO}_2] = 230 \mu\text{M}$, $[\text{BPA}] = 25 \mu\text{M}$, $\text{pH} = 5.0$. Error bars are determined from the σ -
 6 level uncertainty of the data fit used to obtain k_{BPA} .

7 The effects of Mn^{2+} concentrations on the degradation of BPA were studied as well. Fig. 2(b)
 8 shows that with the addition of Mn^{2+} from 2 to $20 \mu\text{M}$, the k_{BPA} was increased from 0.0246 to

1 0.0398 min⁻¹. The improved removal of BPA can be attributed to the formation of more
2 Mn(III)-PP complexes with the increase of Mn²⁺ concentrations. The k_{BPA} at 0 μM of Mn²⁺
3 was excluded from this comparison due to the fact that the degradation of BPA by the
4 MnO₂/PP system in the absence of Mn²⁺ does not obey the pseudo-first-order rate (Fig. 1). In
5 order to minimize the environmental toxicity associated with higher Mn²⁺ concentrations, a
6 concentration of 10 μM was deemed appropriate for subsequent experiments, even though
7 larger quantities of Mn²⁺ have been shown to enhance BPA degradation. In addition, to ensure
8 all the produced Mn(III) species can be complexed by PP, slight excess of PP concentration
9 (1.2 mM) will be employed in the following steps.

10 **3.3 The primary reactive species**

11 Mn(III)-ligand complexes are considered as the main reactive species for organic pollutants
12 degradation in the ligands-assisted manganese oxide systems [15]. Therefore, in the present
13 study, the formation of Mn(III)-PP complexes in different processes were followed using the
14 UV-visible spectrophotometer. Ten times higher concentrations of all participating chemical
15 compounds were used to measure the formation of Mn(III)-PP complexes due to the low
16 absorption intensity of Mn(III)-PP complexes at 480 nm ($\epsilon = 65 \text{ M}^{-1} \text{ cm}^{-1}$) [30]. Moreover, the
17 blank experiments were conducted to exclude the possible influence of BPA degradation
18 products on the measurement of Mn(III)-PP complexes (Fig. S2).



1
 2 **Fig. 3.** The formation of Mn(III)-PP complexes in different processes. Experimental
 3 conditions: $[\text{MnO}_2] = 2.3 \text{ mM}$, $[\text{Mn}^{2+}] = 100 \mu\text{M}$, $[\text{PP}] = 12 \text{ mM}$, $[\text{BPA}] = 250 \mu\text{M}$, $\text{pH} = 5.0$.
 4 The relative experimental error lies at 5% for Mn(III)-PP complex.

5 Fig. 3 shows that no obvious formation of Mn(III)-PP complex was observed in the system of
 6 MnO_2 (2.3 mM) and PP (12 mM) in 3 h. It might be attributed to the low concentration of
 7 Mn(III)-PP complex formed in reaction and the low absorbance intensity of Mn(III)-PP
 8 complex at 480 nm. To verify whether Mn(III)-PP complexes were really generated in the
 9 reaction of MnO_2 and PP, the absorbance signals of complex at 258 nm were checked (258
 10 and 480 nm are two absorbance peaks of Mn(III)-PP complex on UV-Vis spectrum). As
 11 shown in Fig. S3, the absorbance intensity of Mn(III)-PP complex at 258 nm slightly
 12 increased with the reaction time, indicating the formation of Mn(III)-PP complexes. However,
 13 the increased scale of Mn(III)-PP complexes absorbance is small (~ 0.01 in 3 h). This can be
 14 explained by the low reactivity of MnO_2 with PP for the generation of Mn(III)-PP complexes.
 15 Similar results were reported by Liu et al.. They found that $\delta\text{-MnO}_2$ (0.01 g L^{-1}) takes three
 16 days to form $15.6 \mu\text{M}$ of Mn(III)-PP complexes with 5 mM PP [16]. The low performance of
 17 MnO_2 for PP complexation at low solution pH can be attributed to the strong electrostatic

1 repulsion between them. The point of zero charges (PZC) of MnO_2 is 2.3-2.9, thus the surface
2 of MnO_2 is filled with negative charges at solution pH 5.0 [31]. The pKa values of PP are
3 0.85, 1.96, 6.60, and 9.41, resulting in a negatively charged PP ($\text{H}_2\text{P}_2\text{O}_7^{2-}$) at pH 5.0 [32].
4 Therefore, the contact between MnO_2 and PP at pH 5.0 is weak, leading to the slow
5 generation of the Mn(III)-PP complexes.

6 In the presence of Mn^{2+} (100 μM), the generation of Mn(III)-PP complex by the MnO_2 /PP
7 system was much more rapid ($\sim 125 \mu\text{M}$ Mn(III)-PP complexes were formed in 30 min). The
8 results clearly show the positive role of Mn^{2+} in catalyzing MnO_2 in the presence of PP. As
9 discussed above, in the acid environment, the reaction between MnO_2 and PP will be
10 suppressed due to the occurrence of electrostatic repulsion. However, with the addition of
11 positively charged Mn^{2+} , the negative charges on the surface of MnO_2 (especially the
12 vacancies sites) will be neutralized. Therefore, the presence of Mn^{2+} can significantly improve
13 the adsorption of PP by MnO_2 , leading to the accelerated generation of Mn(III)-PP complexes.
14 However, it is worth noting that no more Mn(III)-PP complex was generated after 30 min
15 reaction in the system of MnO_2 /PP/ Mn^{2+} . This result can be attributed to the missing of
16 reductants (such as BPA) which are necessary for the cyclic generation of Mn(III) species.

17 In comparison, in the presence of BPA, the amount of Mn(III)-PP complexes generated in the
18 MnO_2 /PP system was increased ($\sim 800 \mu\text{M}$ in 3 h). The result can be explained by the fact that
19 BPA as a reductant was oxidized by high valent Mn species (e.g., Mn(IV) and Mn(III)),
20 leading to the generation of byproducts (BPA_{ox}) and Mn^{2+} . The generated Mn^{2+} can
21 participate in the reaction of MnO_2 and PP accelerating the formation of Mn(III)-PP
22 complexes. Fig. S4 shows the removal efficiency of BPA was improved with the increase of
23 the concentrations of Mn(III)-PP complexes. However, it is worth noting that in the first 30
24 min, the formation rate and amount of Mn(III)-PP complexes in the MnO_2 /PP/BPA processes

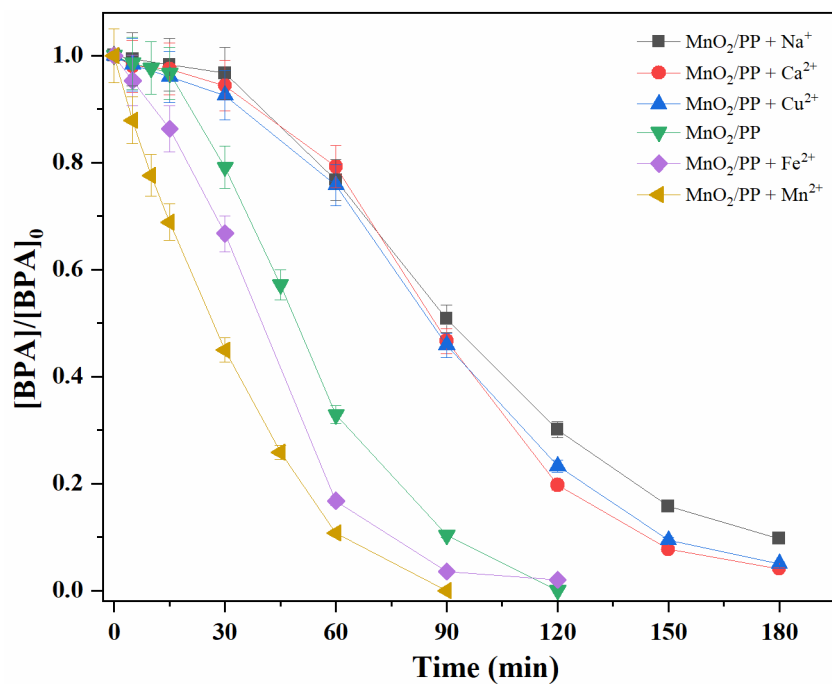
1 are very low ($\sim 36.7 \mu\text{M}$) (Fig. 3), indicating the existence of an induction period of BPA
2 degradation by the MnO_2/PP system. The result is consistent with the degradation tendency of
3 BPA in the MnO_2/PP system (Fig. 1).

4 Moreover, it is easy to see that the amount of Mn(III)-PP complexes generated in the
5 $\text{MnO}_2/\text{PP}/\text{Mn}^{2+}$ system in the first 30 min is higher than that in the $\text{MnO}_2/\text{PP}/\text{BPA}$ system
6 (Fig. 3). The results indicate that Mn^{2+} is better than BPA at activating MnO_2 even though
7 both Mn^{2+} and BPA can react with MnO_2 to generate Mn(III) species. This conclusion was
8 confirmed by the results that a higher generation rate of Mn(III)-PP complexes was achieved
9 in the $\text{MnO}_2/\text{PP}/\text{BPA}$ process with the addition of Mn^{2+} ($\sim 250 \mu\text{M}$ Mn(III)-PP complexes
10 generated in 30 min) (Fig. 3). Additionally, the cycle between Mn species (e.g. Mn^{2+} , Mn(III),
11 and Mn(IV)) is favored due to the presence of BPA in the $\text{MnO}_2/\text{PP}/\text{Mn}^{2+}$ system. The
12 amount of Mn(III)-PP complexes formed in the $\text{MnO}_2/\text{PP}/\text{Mn}^{2+}/\text{BPA}$ system ($\sim 1000 \mu\text{M}$ in 3
13 h) is much higher than that in the $\text{MnO}_2/\text{PP}/\text{Mn}^{2+}$ process ($125 \mu\text{M}$). In summary, Mn(III)-PP
14 complexes are the main reactive species for the efficient degradation of BPA by the
15 $\text{MnO}_2/\text{PP}/\text{Mn}^{2+}$ system. Moreover, Mn^{2+} plays an important role in BPA degradation by PP-
16 assisted MnO_2 .

17 **3.4 The role of Mn^{2+}**

18 In previous research, greater emphasis has been placed on the role of Mn(III) in the reactivity
19 of MnO_2 , while the contribution of Mn^{2+} has been overlooked. In the present study, the
20 multiple roles of Mn^{2+} in BPA degradation by the PP-assisted MnO_2 system were investigated
21 in detail. Firstly, positively charged Mn^{2+} acts as a role of bridge to increase the connection
22 between MnO_2 and PP. The results can be explained by the naturally electrostatic adsorption.
23 This conclusion is supported by the study of Wang et al. that reported the adsorption of fulvic
24 acid by MnO_2 was enhanced with the addition of divalent cations [33]. However, it is worth

1 noting that the formation of MnO₂-metal cations-PP bridge does not equally imply the
2 degradation of organic pollutants can be improved. For example, Fig. 4 shows that adding
3 Na⁺, Ca²⁺, and Cu²⁺ inhibited the removal of BPA by PP-assisted MnO₂. It can be explained
4 by the fact that the presence of Na⁺, Ca²⁺, and Cu²⁺ blocked the direct association of PP and
5 Mn²⁺ with MnO₂ leading to the reduced generation of Mn(III)-PP complexes. Therefore,
6 constructing an effective bridge is the key step for improving the degradation of organic
7 pollutants in the MnO₂/PP system. Comparing to Na⁺, Ca²⁺, and Cu²⁺, Mn²⁺ is more
8 susceptible to be oxidized by MnO₂ to form higher valent Mn ions due to the high redox
9 potential of MnO₂ ($E_{\text{MnO}_2/\text{Mn}^{2+}}^0 = 1.24 \text{ V vs NHE}$) [6]. Thus, the reductive activity of Mn²⁺
10 could be the reason that Mn²⁺ are able to improve the degradation of BPA in the MnO₂/PP
11 system while Na⁺, Ca²⁺, and Cu²⁺ cannot. To verify this hypothesis, ferrous ion ($E_{\text{Fe}^{3+}/\text{Fe}^{2+}}^0 =$
12 0.771 V vs NHE) as a substitute of Mn²⁺ was added in the reaction and the removal efficiency
13 of BPA by the MnO₂/PP system was monitored [34]. As shown in Fig. 4, the addition of Fe²⁺
14 was obviously improved the degradation rate of BPA in the system of MnO₂/PP. Therefore,
15 the successful bridge should be established on the reductive metal ions which can be oxidized
16 by MnO₂. In addition, Mn²⁺ also exhibited the catalytic effect on the reactivity of MnO₂ in the
17 presence of PP. This conclusion can be verified by several phenomenon. For instance, the
18 induction period existed in the degradation of BPA by MnO₂/PP was disappeared in the
19 presence of Mn²⁺ (Fig. 4). Moreover, the amounts and the generation rates of Mn(III)-PP
20 complexes were obviously improved in the MnO₂/PP system due to the addition of Mn²⁺ (Fig.
21 3). In summary, Mn²⁺ ion presented multiple roles, including bridging, reductive, and
22 catalytic roles, which significantly enhance the degradation of BPA by MnO₂ in the presence
23 of PP.

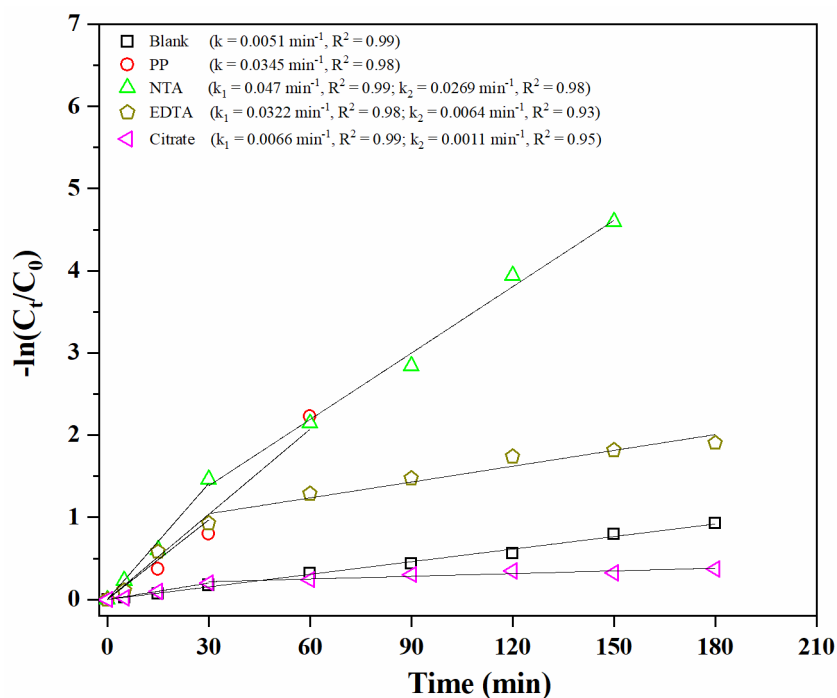


1
2 **Fig. 4.** BPA degradation by the MnO₂/PP system in the presence of various metal cations.
3 Experimental conditions: [MnO₂] = 230 μM, [ligands] = 1.2 mM, [BPA] = 25 μM, [Metal
4 cations] = 10 μM, pH = 5.0. The relative experimental error lies at 5% for BPA.

5

6 3.5 Effect of ligand types

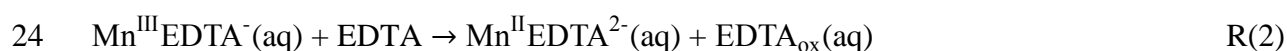
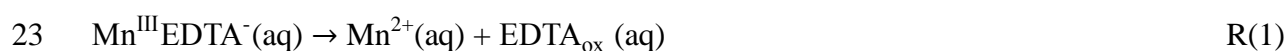
7 In order to study the effect of different ligands on the degradation of BPA in the MnO₂/Mn²⁺
8 system, three other common ligands (i.e., NTA, EDTA, and Citrate) were employed to
9 activate the MnO₂/Mn²⁺ system.



1
 2 **Fig. 5.** Kinetic analysis of BPA degradation by $\text{MnO}_2/\text{ligands}/\text{Mn}^{2+}$ system using pseudo-
 3 first-order model. Experimental conditions: $[\text{MnO}_2] = 230 \mu\text{M}$, $[\text{ligands}] = 1.2 \text{ mM}$, $[\text{BPA}] =$
 4 $25 \mu\text{M}$, $[\text{Mn}^{2+}] = 10 \mu\text{M}$, $\text{pH} = 5.0$.

5 The degradation efficiency of BPA by various ligands-assisted MnO_2 system is shown in Fig.
 6 S5. To better demonstrate the kinetic of BPA degradation by MnO_2 in the presence of
 7 different ligands, the variation of $-\ln(C_t/C_0)$ vs time was depicted in Fig. 5. It can be seen that
 8 without the addition of ligands, the degradation of BPA by the $\text{MnO}_2/\text{Mn}^{2+}$ system obeys the
 9 pseudo-first-order rate where the k_{BPA} is 0.0051 min^{-1} . However, the addition of different
 10 types of ligands leads to various BPA degradation kinetics. For example, in the presence of
 11 PP (a non redox-type ligand), the removal of BPA by the $\text{MnO}_2/\text{Mn}^{2+}$ system followed the
 12 pseudo-first-order rate. In comparison, with the addition of organic types ligands (e.g., NTA
 13 and EDTA), the processes of BPA degradation by the $\text{MnO}_2/\text{ligand}/\text{Mn}^{2+}$ systems were
 14 separated into acceleration and deceleration parts. In the first 30 min, the presence of NTA
 15 and EDTA obviously accelerated the degradation of BPA by $\text{MnO}_2/\text{Mn}^{2+}$ with the k_{BPA} of
 16 0.0470 min^{-1} and 0.0322 min^{-1} , respectively. However, after 30 min, the kinetics of BPA
 17 removal were decelerated. Especially for the EDTA used as organic ligand, after 30 min of

1 reaction, the k_{BPA} was decreased to 0.0064 min^{-1} which is close to the reaction rate of the
 2 blank process. The observed high k_{BPA} values in the first 30 min can be attributed to the
 3 generation of high amounts of Mn(III)-NTA and Mn(III)-EDTA complexes due to the higher
 4 stability constants of the complexes (as shown in Table S2). The decreased k_{BPA} after 30 min
 5 reaction can be explained by the rapid decomposition of Mn(III)-NTA and Mn(III)-EDTA
 6 complexes via different pathways. For instance, it is reported that Mn(III)-EDTA complexes
 7 can be decomposed through the inter- or intra- molecular electron transfers as shown in R(1)
 8 and R(2) [17,27]. Moreover, the same authors reported that the half-life time of Mn(III)-
 9 EDTA decomposition with the molar ratio of $[\text{Mn}]/[\text{EDTA}]$ 1:50 is less than 10 min in the pH
 10 range of 5.0-6.0 [27]. The variation of the absorbance intensity of Mn(III)-EDTA vs time was
 11 followed (Fig. S6). The absorbance rapidly increased and reached its maximum value of
 12 approximately 0.0095 after 30 minutes, followed by a gradual decline. These results indicate
 13 the formation and accumulation of Mn(III)-EDTA complex during the initial 30 minutes,
 14 followed by its gradual consumption. In addition, NTA and EDTA as the organic ligands can
 15 directly consume MnO_2 through the redox processes resulting in the decrease of BPA
 16 degradation [35]. The low efficiency of citrate on the reactivity of MnO_2 verified this point as
 17 well. It is clear to see that the occurrence of citrate did not improve the degradation of BPA by
 18 the $\text{MnO}_2/\text{Mn}^{2+}$ system. Even, the presence of citrate slightly inhibited the removal of BPA by
 19 the $\text{MnO}_2/\text{Mn}^{2+}$ system after 30 min reaction. In conclusion, the addition of PP can facilitate
 20 the degradation of organic pollutants by MnO_2 in the presence of Mn^{2+} . However, the
 21 performance of organic ligands (e.g., EDTA, NTA) on the reactivity of MnO_2 depends on the
 22 stability of the complex.

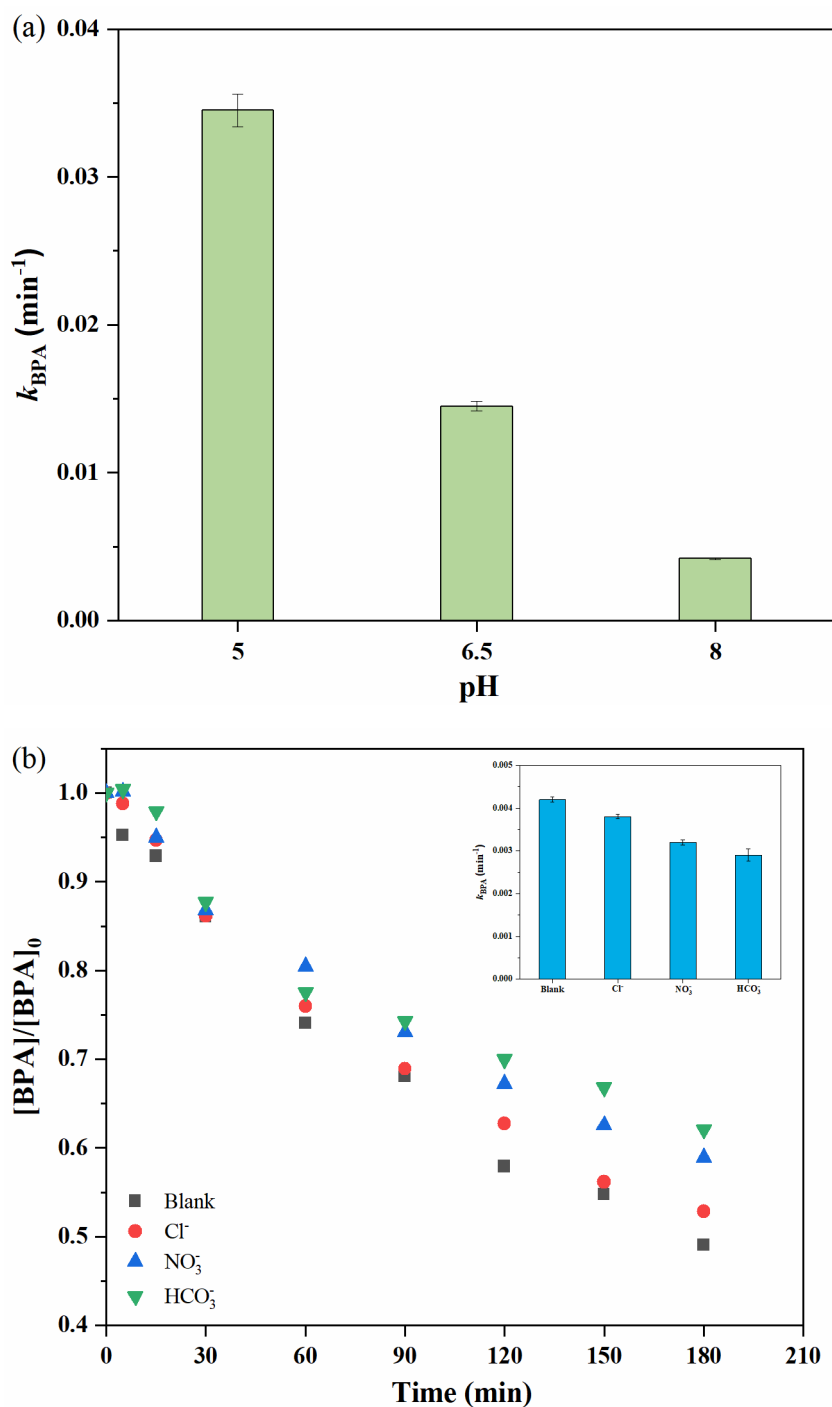


1

2 3.6 Effects of solution pH and inorganic anions

3 The effects of solution pH and inorganic ions were investigated to evaluate the adaptability of
4 the $\text{MnO}_2/\text{PP}/\text{Mn}^{2+}$ system in a natural aquatic environment.

5



6

7 **Fig. 6.** BPA degradation by $\text{MnO}_2/\text{PP}/\text{Mn}^{2+}$. (a) Effect of solution pH. (b) Effect of inorganic

8 anions at initial pH 8.0 (insert: kinetic constants of BPA degradation in the absence and

1 presence of various inorganic anions). Experimental conditions: $[\text{MnO}_2] = 230 \mu\text{M}$, $[\text{PP}] = 1.2$
2 mM , $[\text{BPA}] = 25 \mu\text{M}$, $[\text{Mn}^{2+}] = 10 \mu\text{M}$, $[\text{Cl}^-] = [\text{NO}_3^-] = [\text{HCO}_3^-] = 0.5 \text{ mM}$. Error bars are
3 determined from the σ -level uncertainty of the data fit used to obtain k_{BPA} .

4 As shown in Fig. 6 (a), the kinetic constants of BPA degradation at pH 6.5 and 8.0 are 0.0145
5 and 0.0042 min^{-1} separately, which are lower than the k_{BPA} achieved at pH 5.0. The results
6 can be attributed to the low oxidative reactivities of MnO_2 and Mn(III)-PP complexes at high
7 solution pH. As discussed in *section 3.3*, BPA can be directly oxidized by MnO_2 , and the
8 generated Mn(III) species promotes the degradation of BPA with the assistance of PP.

9 Moreover, based on the previous report, increasing solution pH from 4.0 to 8.0 leads to the
10 reductive potential of MnO_2 decreasing from 0.99 to 0.76 V [28]. Therefore, both the direct
11 oxidation of BPA by MnO_2 and the amounts of Mn(III) species generated in the reaction will
12 be reduced at higher solution pH. Furthermore, the oxidative reactivity of Mn(III)-PP
13 complex under different solution pH needs to be considered since the complexes are the main
14 reactive species for BPA degradation in the $\text{MnO}_2/\text{PP}/\text{Mn}^{2+}$ system. Fig. S7 shows that
15 increasing solution pH from 5.0 to 8.0, the degradation efficiency of BPA by Mn(III)-PP
16 complexes at 5 min was decreased from 65% to 35 %. Thus, considering both the reactivity of
17 MnO_2 and Mn(III)-PP complex, the decrease of k_{BPA} at higher solution pH is understandable.

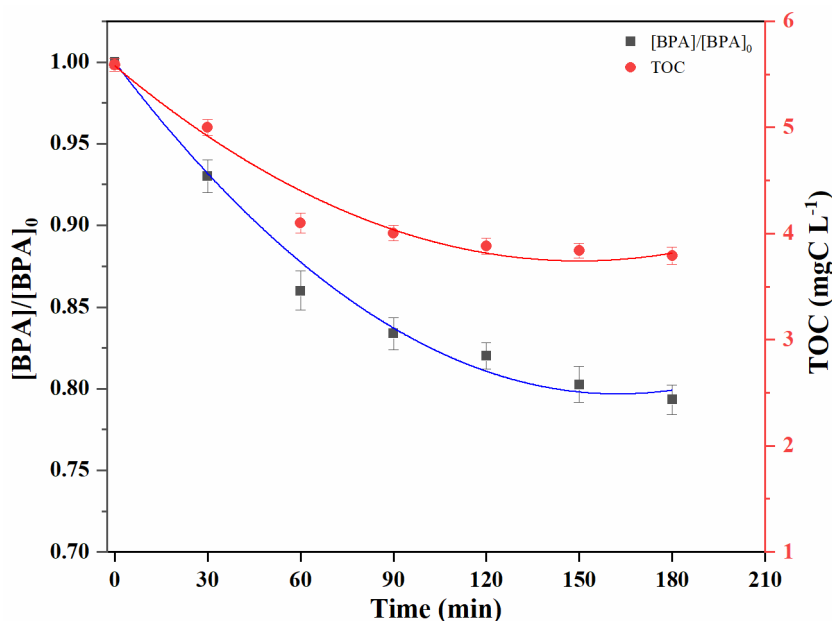
18 Inorganic anions such as Cl^- , NO_3^- , and HCO_3^- are commonly found in wastewater. The
19 removal of organic pollutants by the advanced oxidation processes (AOPs) is usually
20 disturbed by the presence of inorganic anions [36]. The effect of inorganic anions on the
21 degradation of BPA by the $\text{MnO}_2/\text{PP}/\text{Mn}^{2+}$ system under solution pH 8.0 was investigated.

22 Fig. 6 (b) shows that the addition of inorganic anions (e.g., Cl^- , NO_3^- , and HCO_3^-) slightly
23 inhibited the removal of BPA by the $\text{MnO}_2/\text{PP}/\text{Mn}^{2+}$ system. In the presence of Cl^- , NO_3^- , and
24 HCO_3^- , the k_{BPA} (0.0042 min^{-1}) was decreased to 0.0038, 0.0032, and 0.0029 min^{-1} ,

1 respectively. The results might be explained by the competition between inorganic anions and
2 negatively charged PP species for the connection to Mn^{2+} adsorbed on the surface of MnO_2 .

3 3.7 Assessing the degradation of BPA in STP outlet water

4 To assess the performance of the $\text{MnO}_2/\text{PP}/\text{Mn}^{2+}$ system in treating real wastewater, the
5 removal of BPA by the $\text{MnO}_2/\text{PP}/\text{Mn}^{2+}$ system in the sewage treatment plant (STP) outlet
6 water was evaluated.



7
8 **Fig. 7.** BPA degradation efficiency and TOC removal in STP outlet water by the
9 $\text{MnO}_2/\text{PP}/\text{Mn}^{2+}$ system. Experimental conditions: $[\text{MnO}_2] = 230 \mu\text{M}$, $[\text{PP}] = 1.2 \text{ mM}$, $[\text{BPA}]$
10 $= 25 \mu\text{M}$, $[\text{Mn}^{2+}] = 10 \mu\text{M}$, $\text{pH} = 8.0$. The solid lines show the fit of data using a polynomial
11 function.

12 The initial total organic carbon (TOC) was measured to be 5.59 mgC L^{-1} (where 3.86 mgC L^{-1}
13 comes from adding BPA). Fig. 7 shows the degradation of BPA by the $\text{MnO}_2/\text{PP}/\text{Mn}^{2+}$ system
14 in the STP outlet water was inhibited ($\sim 20\%$ removal in 3 h) compared with the pure water
15 results. Around 1.49 mgC L^{-1} of TOC was removed by the $\text{MnO}_2/\text{PP}/\text{Mn}^{2+}$ system in the first
16 1 h, however in the following 2 h, only 0.31 mgC L^{-1} of TOC was degraded. The results can
17 be attributed to the presence of inorganic anions, organic matter, and metal ions in the STP

1 outlet water. Table S1 shows 62.93 mgC L⁻¹ of inorganic carbon and various anions such as
2 Cl⁻, NO₃⁻, and SO₄²⁻ were present in the STP outlet water. The negative effect of inorganic
3 anions on the MnO₂/PP/Mn²⁺ system has been discussed in *section 3.6*. Moreover, it is known
4 that organic matter can compete with organic pollutants (e.g., BPA) for the reactive species
5 which are generated in the reaction. Thus, the presence of 1.73 mgC L⁻¹ of organic carbon in
6 the employed STP outlet water will inhibit the degradation of BPA by the MnO₂/PP/Mn²⁺
7 system. In addition, the presence of various less-reductive cations further blocked the
8 formation of Mn(III)-PP complexes in the MnO₂/PP/Mn²⁺ system leading to the suppressed
9 degradation of BPA as discussed in *section 3.4*.

10

11 **4 Conclusion**

12 Mn(III)-mediated organic contaminants degradation have attracted an increasing attention.
13 Many efforts have been taken to increase the amount of Mn(III) species during the processes
14 of organic compound oxidation by the manganese oxides. In comparison to previous, the role
15 of Mn²⁺ in enhancing the reactivity of manganese oxides is studied in detail. In this study, the
16 efficiency and mechanism of BPA degradation by the MnO₂/PP/Mn²⁺ system was
17 investigated. 25 μM of BPA was completely removed by the MnO₂/PP/Mn²⁺ system in 90
18 min. Mn(III)-PP complexes were verified as the primary reactive species for BPA oxidation.
19 Moreover, Mn²⁺ was demonstrated to be an important compound for the final efficiency and
20 to act bridging, reductive, and catalytic roles in the MnO₂/PP/Mn²⁺ system. The substituted
21 ligands such as EDTA and NTA demonstrated superior performance in activating MnO₂
22 within a restricted timeframe, while citrate was found to have an insignificant impact on the
23 degradation of BPA. The results of the investigation also indicate that the MnO₂/PP/Mn²⁺
24 system exhibits a preference for oxidizing BPA under acidic conditions. Furthermore, close to
25 natural pH around 8, the presence of inorganic ions such as chloride, nitrate, and bicarbonate

1 ions exhibited only a slight inhibition on the degradation of BPA by the $\text{MnO}_2/\text{PP}/\text{Mn}^{2+}$
2 system. Furthermore, the application of the proposed system in the sewage treatment plant
3 outlet water was found to be inhibited due to the presence of organic matters, inorganic anions,
4 and metal cations. The findings of this research provide comprehensive insights into the role
5 of Mn^{2+} in the ligand-assisted MnO_2 system and serve as a valuable reference for
6 understanding the degradation of organic pollutants by manganese dioxide in the natural
7 environment.

8
9
10
11
12

13 **Credit authorship contribution statement**

14 **Daqing Jia:** Conceptualization, Methodology, Investigation, Writing-Original Draft

15 **Marcello Brigante:** Resources, Writing-Review & Editing

16 **Changbo Zhang:** Formal analysis, Methodology

17 **Gilles Mailhot:** Conceptualization, Supervision, Writing-Review & Editing

18

19 **Declaration of competing interest**

20 The authors declare that they have no known competing financial interests or personal
21 relationships that could have appeared to influence the work reported in this paper.

22

23 **Acknowledgements**

24 The work was supported by the “Fédération des Recherches en Environnement” (FR CNRS)
25 and the I-Site project CAP 20-25 of University Clermont Auvergne (UCA). This work also
26 financed by the Foreign Experts Program of the Ministry of Science and Technology of the
27 people’s Republic of China (No. G2022051018L). The authors gratefully acknowledge
28 financial support from China Scholarship Council provided to Daqing Jia (No, 201806920034)
29 to study at the University Clermont Auvergne in Clermont-Ferrand, France.

1
2
3
4
5
6
7
8
9
10
11
12
13
14
15
16
17
18
19
20
21
22
23
24
25
26
27
28
29
30
31
32
33
34
35
36
37
38

References

- [1]X. Wang, G.-J. Xie, N. Tian, C.-C. Dang, C. Cai, J. Ding, B.-F. Liu, D.-F. Xing, N.-Q. Ren, Q. Wang, Anaerobic microbial manganese oxidation and reduction: A critical review, *Sci. Total Environ.* 822 (2022) 153513. <https://doi.org/10.1016/j.scitotenv.2022.153513>.
- [2]Y. Tu, G. Shao, W. Zhang, J. Chen, Y. Qu, F. Zhang, S. Tian, Z. Zhou, Z. Ren, The degradation of printing and dyeing wastewater by manganese-based catalysts, *Sci. Total Environ.* 828 (2022) 154390. <https://doi.org/10.1016/j.scitotenv.2022.154390>.
- [3]S.-L. Chiam, S.-Y. Pung, F.Y. Yeoh, M. Ahmadipour, Highly efficient oxidative degradation of organic dyes by manganese dioxide nanoflowers, *Mater. Chem. Phys.* 280 (2022) 125848. <https://doi.org/10.1016/j.matchemphys.2022.125848>.
- [4]J. Huang, S. Zhong, Y. Dai, C.-C. Liu, H. Zhang, Effect of MnO₂ Phase Structure on the Oxidative Reactivity toward Bisphenol A Degradation, *Environ. Sci. Technol.* 52 (2018) 11309–11318. <https://doi.org/10.1021/acs.est.8b03383>.
- [5]D. Jia, O. Monfort, K. Hanna, G. Mailhot, M. Brigante, Caffeine degradation using peroxydisulfate and peroxymonosulfate in the presence of Mn₂O₃. Efficiency, reactive species formation and application in sewage treatment plant water, *J. Clean. Prod.* 328 (2021) 129652. <https://doi.org/10.1016/j.jclepro.2021.129652>.
- [6]K.S. Yamaguchi, D.T. Sawyer, The Redox Chemistry of Manganese(III) and -(IV) Complexes, *Isr. J. Chem.* 25 (1985) 164–176. <https://doi.org/10.1002/ijch.198500026>.
- [7]R.J. Watts, J. Sarasa, F.J. Loge, A.L. Teel, Oxidative and Reductive Pathways in Manganese-Catalyzed Fenton’s Reactions, *J. Environ. Eng.* 131 (2005) 158–164. [https://doi.org/10.1061/\(ASCE\)0733-9372\(2005\)131:1\(158\)](https://doi.org/10.1061/(ASCE)0733-9372(2005)131:1(158)).
- [8]J. Huang, Y. Dai, K. Singewald, C.-C. Liu, S. Saxena, H. Zhang, Effects of MnO₂ of different structures on activation of peroxymonosulfate for bisphenol A degradation under acidic conditions, *Chem. Eng. J.* 370 (2019) 906–915. <https://doi.org/10.1016/j.cej.2019.03.238>.
- [9]D. Jia, Q. Li, K. Hanna, G. Mailhot, M. Brigante, Efficient removal of estrogenic compounds in water by Mn(III)-activated peroxymonosulfate: Mechanisms and application in sewage treatment plant water, *Environ. Pollut.* 288 (2021) 117728. <https://doi.org/10.1016/j.envpol.2021.117728>.
- [10]E. Domingues, M.J. Silva, T. Vaz, J. Gomes, R.C. Martins, Sulfate radical based advanced oxidation processes for agro-industrial effluents treatment: A comparative review with Fenton’s peroxidation, *Sci. Total Environ.* 832 (2022) 155029. <https://doi.org/10.1016/j.scitotenv.2022.155029>.

- 1 [11]Y. Zhang, M. Zhou, A critical review of the application of chelating agents to enable
2 Fenton and Fenton-like reactions at high pH values, *J. Hazard. Mater.* 362 (2019) 436–450.
3 <https://doi.org/10.1016/j.jhazmat.2018.09.035>.
- 4 [12]D. Jia, S.-P. Sun, Z. Wu, N. Wang, Y. Jin, W. Dong, X.D. Chen, Q. Ke, TCE degradation
5 in groundwater by chelators-assisted Fenton-like reaction of magnetite: Sand columns
6 demonstration, *J. Hazard. Mater.* 346 (2018) 124–132.
7 <https://doi.org/10.1016/j.jhazmat.2017.12.031>.
- 8 [13]Y. Gao, Y. Zhou, S.-Y. Pang, J. Jiang, Y.-M. Shen, Y. Song, J.-B. Duan, Q. Guo,
9 Enhanced peroxydisulfate activation via complexed Mn(II): A novel non-radical oxidation
10 mechanism involving manganese intermediates, *Water Res.* 193 (2021) 116856.
11 <https://doi.org/10.1016/j.watres.2021.116856>.
- 12 [14]Y. Gao, J. Jiang, Y. Zhou, S.-Y. Pang, C. Jiang, Q. Guo, J.-B. Duan, Does Soluble
13 Mn(III) Oxidant Formed in Situ Account for Enhanced Transformation of Triclosan by
14 Mn(VII) in the Presence of Ligands?, *Environ. Sci. Technol.* 52 (2018) 4785–4793.
15 <https://doi.org/10.1021/acs.est.8b00120>.
- 16 [15]W. Qin, P. Tan, Y. Song, Z. Wang, J. Nie, J. Ma, Enhanced transformation of phenolic
17 compounds by manganese(IV) oxide, manganese(II) and permanganate in the presence of
18 ligands: The determination and role of Mn(III), *Sep. Purif. Technol.* 261 (2021) 118272.
19 <https://doi.org/10.1016/j.seppur.2020.118272>.
- 20 [16]W. Liu, B. Sun, J. Qiao, X. Guan, Influence of Pyrophosphate on the Generation of
21 Soluble Mn(III) from Reactions Involving Mn Oxides and Mn(VII), *Environ. Sci. Technol.* 53
22 (2019) 10227–10235. <https://doi.org/10.1021/acs.est.9b03456>.
- 23 [17]C.S. Mc Ardell, A.T. Stone, J. Tian, Reaction of EDTA and Related Aminocarboxylate
24 Chelating Agents with CoIIIIOOH (Heterogenite) and MnIIIIOOH (Manganite), *Environ. Sci.*
25 *Technol.* 32 (1998) 2923–2930. <https://doi.org/10.1021/es980362v>.
- 26 [18]J.E. Post, Manganese oxide minerals: Crystal structures and economic and environmental
27 significance, *Proc. Natl. Acad. Sci.* 96 (1999) 3447–3454.
28 <https://doi.org/10.1073/pnas.96.7.3447>.
- 29 [19]E.J. Elzinga, Reductive Transformation of Birnessite by Aqueous Mn(II), *Environ. Sci.*
30 *Technol.* 45 (2011) 6366–6372. <https://doi.org/10.1021/es2013038>.
- 31 [20]J.P. Lefkowitz, A.A. Rouff, E.J. Elzinga, Influence of pH on the Reductive
32 Transformation of Birnessite by Aqueous Mn(II), *Environ. Sci. Technol.* 47 (2013) 10364–
33 10371. <https://doi.org/10.1021/es402108d>.
- 34 [21]H. Cheng, T. Yang, J. Jiang, X. Lu, P. Wang, J. Ma, Mn²⁺ effect on manganese oxides
35 (MnO_x) nanoparticles aggregation in solution: Chemical adsorption and cation bridging,
36 *Environ. Pollut.* 267 (2020) 115561. <https://doi.org/10.1016/j.envpol.2020.115561>.
- 37 [22]W. Huang, G. Wu, H. Xiao, H. Song, S. Gan, S. Ruan, Z. Gao, J. Song, Transformation
38 of m-aminophenol by birnessite (δ-MnO₂) mediated oxidative processes: Reaction kinetics,
39 pathways and toxicity assessment, *Environ. Pollut.* 256 (2020) 113408.
40 <https://doi.org/10.1016/j.envpol.2019.113408>.

- 1 [23]Y. Sun, C. Wang, A.L. May, G. Chen, Y. Yin, Y. Xie, A.M. Lato, J. Im, F.E. Löffler,
2 Mn(III)-mediated bisphenol a degradation: Mechanisms and products, *Water Res.* 235 (2023)
3 119787. <https://doi.org/10.1016/j.watres.2023.119787>.
- 4 [24]W. Zong, Z. Guo, M. Wu, X. Yi, H. Zhou, S. Jing, J. Zhan, L. Liu, Y. Liu, Synergistic
5 multiple active species driven fast estrone oxidation by δ -MnO₂ in the existence of methanol,
6 *Sci. Total Environ.* 761 (2021) 143201. <https://doi.org/10.1016/j.scitotenv.2020.143201>.
- 7 [25]R.M. McKenzie, The synthesis of birnessite, cryptomelane, and some other oxides and
8 hydroxides of manganese, *Mineral. Mag.* 38 (1971) 493–502.
9 <https://doi.org/10.1180/minmag.1971.038.296.12>.
- 10 [26]A. Qian, W. Zhang, C. Shi, C. Pan, D.E. Giammar, S. Yuan, H. Zhang, Z. Wang,
11 Geochemical Stability of Dissolved Mn(III) in the Presence of Pyrophosphate as a Model
12 Ligand: Complexation and Disproportionation, *Environ. Sci. Technol.* 53 (2019) 5768–5777.
13 <https://doi.org/10.1021/acs.est.9b00498>.
- 14 [27]J.K. Klewicki, J.J. Morgan, Kinetic Behavior of Mn(III) Complexes of Pyrophosphate,
15 EDTA, and Citrate, *Environ. Sci. Technol.* 32 (1998) 2916–2922.
16 <https://doi.org/10.1021/es980308e>.
- 17 [28]D. Jia, Q. Li, T. Luo, O. Monfort, G. Mailhot, M. Brigante, K. Hanna, Impacts of
18 environmental levels of hydrogen peroxide and oxyanions on the redox activity of MnO₂
19 particles, *Environ. Sci.: Proc. Imp.* (2021). <https://doi.org/10.1039/D1EM00177A>.
- 20 [29]S. Zhong, H. Zhang, Mn(III)-ligand complexes as a catalyst in ligand-assisted oxidation
21 of substituted phenols by permanganate in aqueous solution, *J. Hazard. Mater.* 384 (2020)
22 121401. <https://doi.org/10.1016/j.jhazmat.2019.121401>.
- 23 [30]S.M. Webb, G.J. Dick, J.R. Bargar, B.M. Tebo, Evidence for the presence of Mn(III)
24 intermediates in the bacterial oxidation of Mn(II), *Proc. Natl. Acad. Sci.* 102 (2005) 5558–
25 5563. <https://doi.org/10.1073/pnas.0409119102>.
- 26 [31]Q. Li, D. Schild, M. Pasturel, J. Lützenkirchen, K. Hanna, Alteration of birnessite
27 reactivity in dynamic anoxic/oxic environments, *J. Hazard. Mater.* 433 (2022) 128739.
28 <https://doi.org/10.1016/j.jhazmat.2022.128739>.
- 29 [32]P. Yadav, O. Blacque, A. Roodt, F. Zelder, Induced fit activity-based sensing: a
30 mechanistic study of pyrophosphate detection with a “flexible” Fe-salen complex, *Inorg.*
31 *Chem. Front.* 8 (2021) 4313–4323. <https://doi.org/10.1039/D1QI00209K>.
- 32 [33]Q. Wang, P. Yang, M. Zhu, Effects of metal cations on coupled birnessite structural
33 transformation and natural organic matter adsorption and oxidation, *Geochim. Cosmochim.*
34 *Ac.* 250 (2019) 292–310. <https://doi.org/10.1016/j.gca.2019.01.035>.
- 35 [34]H. Zhou, H. Zhang, Y. He, B. Huang, C. Zhou, G. Yao, B. Lai, Critical review of
36 reductant-enhanced peroxide activation processes: Trade-off between accelerated Fe³⁺/Fe²⁺
37 cycle and quenching reactions, *Appl. Catal. B: Environ.* 286 (2021) 119900.
38 <https://doi.org/10.1016/j.apcatb.2021.119900>.

1 [35]Y. Wang, A.T. Stone, Reaction of Mn^{III,IV} (hydr)oxides with oxalic acid, glyoxylic acid,
2 phosphonoformic acid, and structurally-related organic compounds, *Geochim. Cosmochim.*
3 *Ac.* 70 (2006) 4477–4490. <https://doi.org/10.1016/j.gca.2006.06.1548>.

4 [36]J. Wang, S. Wang, Effect of inorganic anions on the performance of advanced oxidation
5 processes for degradation of organic contaminants, *Chem. Eng. J.* 411 (2021) 128392.
6 <https://doi.org/10.1016/j.cej.2020.128392>.

7